



Direct satellite measurements of the radiative forcing of long-lived halogenated gases

Simon Whitburn^{1,2}

L. Clarisse¹, H. De Longueville³, P. Coheur¹, C. Clerbaux^{1,4}, A.W. Delcloo²

¹ Université libre de Bruxelles (ULB), BLU-ULB research Center, Spectroscopy, Quantum Chemistry and Atmospheric Remote Sensing (SQUARES), Brussels, Belgium (simon.whitburn@ulb.be)

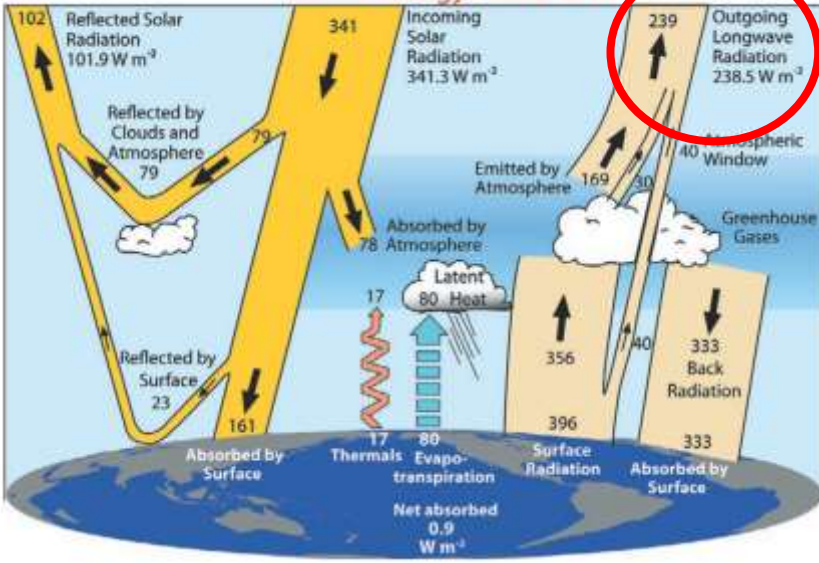
² Royal Meteorological Institute of Belgium (RMIB), Atmospheric Composition, Measurements and Modelling (ACM²), Brussels, Belgium

³ University of Bristol, School of Chemistry, Bristol, United Kingdom

⁴ LATMOS/IPSL, Sorbonne Université, CNRS, Paris, France

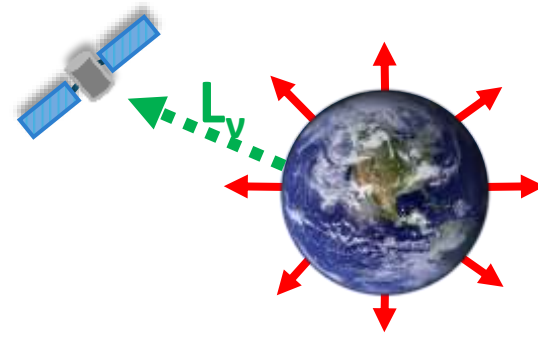


Global Energy Flows $W m^{-2}$



The Earth's Outgoing Longwave Radiation (OLR)

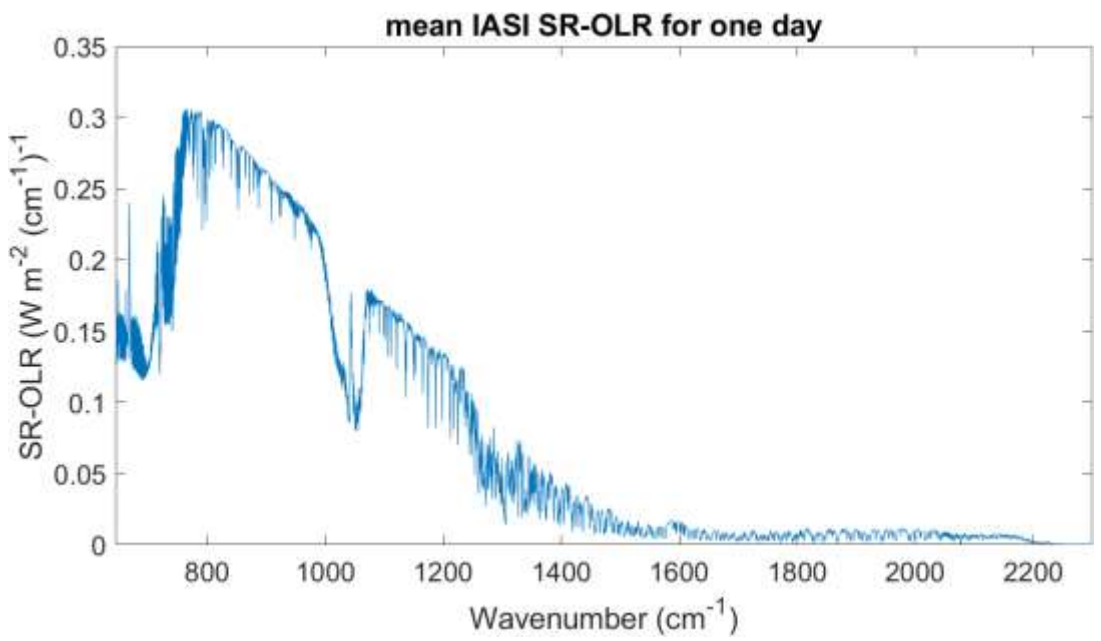
= Total radiation emitted by the Earth-atmosphere system and leaving to space



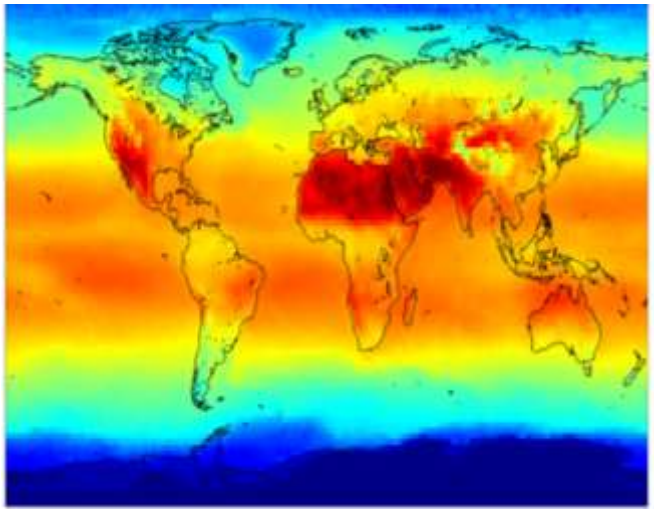
$$F_v = 2\pi \int_0^{\pi/2} L_v(\theta) \sin(\theta) \cos(\theta) d\theta$$

→ A spectrally resolved OLR (SR-OLR) retrieval algorithm from IASI radiances:

$$F_v = \frac{\pi L_v(\theta)}{R_v(\theta)}$$

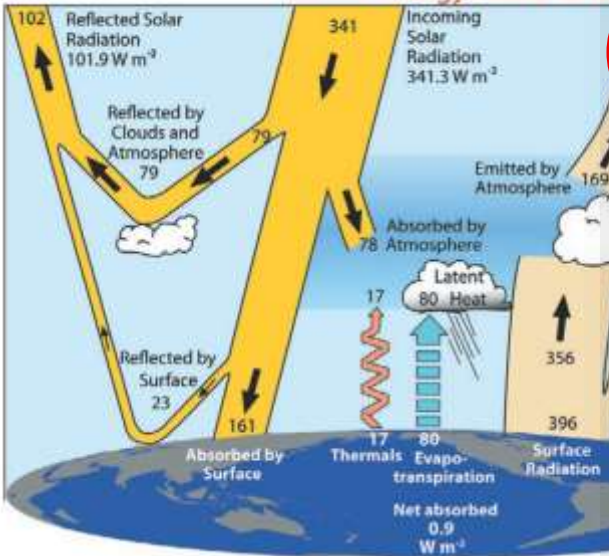


Example of IASI integrated SR-OLR



- For clear-sky scenes
- At the spectral sampling of IASI ($0.25 cm^{-1}$)
- Units: ($W m^{-2} (cm^{-1})^{-1}$)

Excellent fundamental climate data record



Spectrally Resolved Fluxes from IASI Data: Retrieval Algorithm for Clear-Sky Measurements

SIMON WHITBURN,^a LIEVEN CLARISSE,^a SOPHIE BAUDUIN,^a MAYA GEORGE,^b DANIEL HURTMANS,^a SARAH SAFIEDDINE,^b PIERRE FRANÇOIS COHEUR,^a AND CATHY CLERBAUX^b

^a Atmospheric Spectroscopy, Service de Chimie Quantique et Photophysique, Université libre de Bruxelles, Brussels, Belgium

^b LATMOS/IPSL, Sorbonne Université, UVSQ, CNRS, Paris, France

(Manuscript received 17 July 2019, in final form 21 March 2020)

ABSTRACT

Space-based measurements of the outgoing longwave radiation (OLR) are essential for the study of Earth's climate system. While the CERES instrument provides accurate measurements of this quantity, its measurements are not spectrally resolved. Here we present a high-resolution OLR product (sampled at 0.25 cm⁻¹), derived from measurements of the IASI satellite sounder. The applied methodology relies on precalculated angular distribution models (ADMs). These are usually calculated for tens to hundreds of different scene types (characterized by surface and atmosphere parameters). To guarantee accurate results in the range 645–2300 cm⁻¹ covered by IASI, we constructed ADMs for over 140 000 scenes. These were selected from one year of CAMS reanalysis data. A dissimilarity-based selection algorithm was applied to choose scenes as different from each other as possible, thereby maximizing the performance on real data, while keeping the number of scenes manageable. A comparison of the IASI OLR integrated over the 645–2300 cm⁻¹ range was performed with the longwave broadband OLR products from CERES and the AIRS instrument. The latter are systematically higher due to the contribution of the far infrared to the total IR spectral range, but as expected exhibit generally high spatial correlations with the IASI OLR, except for some areas in the tropical region. We also compared the IASI OLR against the spectrally resolved OLR derived from AIRS. A good agreement was found above 1200 cm⁻¹ while AIRS OLR appeared to be systematically higher in the atmospheric window region, likely related to differences in overpass time or to the use of a different cloud detection algorithm.

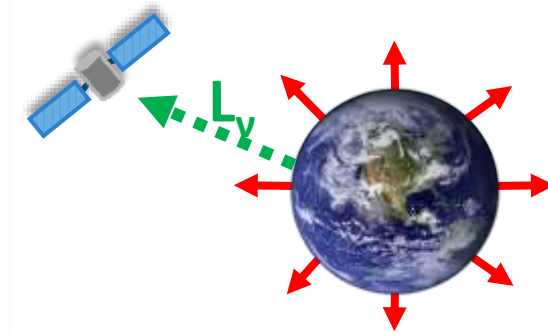
1. Introduction

The top-of-the-atmosphere (TOA) thermal flux, also referred to as Earth's outgoing longwave radiation (OLR) (W m⁻²), represents the total radiation emitted by the Earth–atmosphere system into space. As part of Earth's radiation budget, it reflects how the Earth–atmosphere system balances the incoming solar radiation at the top of the atmosphere and corresponds to about 2/3 of the total outgoing radiation, with the remaining 1/3 being reflected solar radiation (Trenberth et al. 2009). An accurate determination of the OLR is essential to improve our ability to model

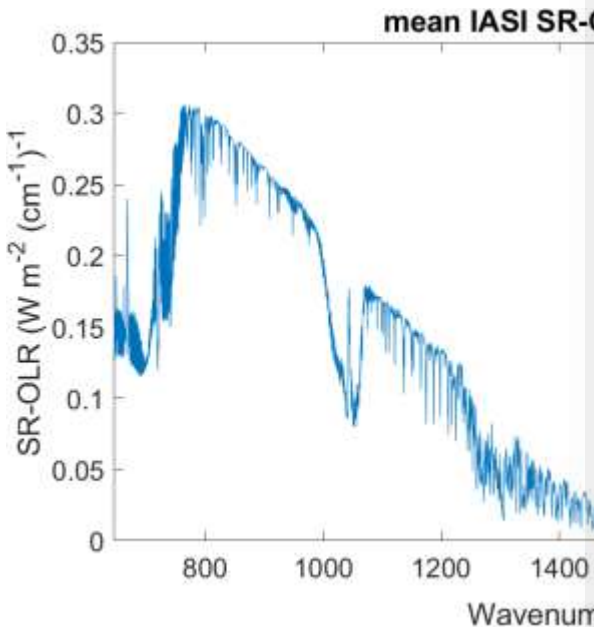
Earth's climate system and to monitor climate feedbacks and processes (Brindley et al. 2015). Since the OLR is affected by clouds, aerosols, water vapor (H₂O), and other greenhouse gases, this requires a good understanding of their impact on Earth's climate. Despite the numerous studies achieved in the last decades (e.g., Soden et al. 2005; Anderson et al. 2010; Y. Huang et al. 2010; Feldman et al. 2011), uncertainties up to a few percent remain, especially for net TOA integrated fluxes (e.g., Loeb et al. 2009; Trenberth et al. 2009; Stephens et al. 2012; Wild et al. 2014).

In principle, infrared sounding satellites are ideal for

ve Radiation



→ A spectrally resolved



$$F_v = \frac{\pi L_v(\theta)}{R_v(\theta)}$$

For clear-sky scenes
 At the spectral sampling of IASI
 (0.25 cm⁻¹)
Units: (W m⁻² (cm⁻¹)⁻¹)

Excellent fundamental
 climate data record

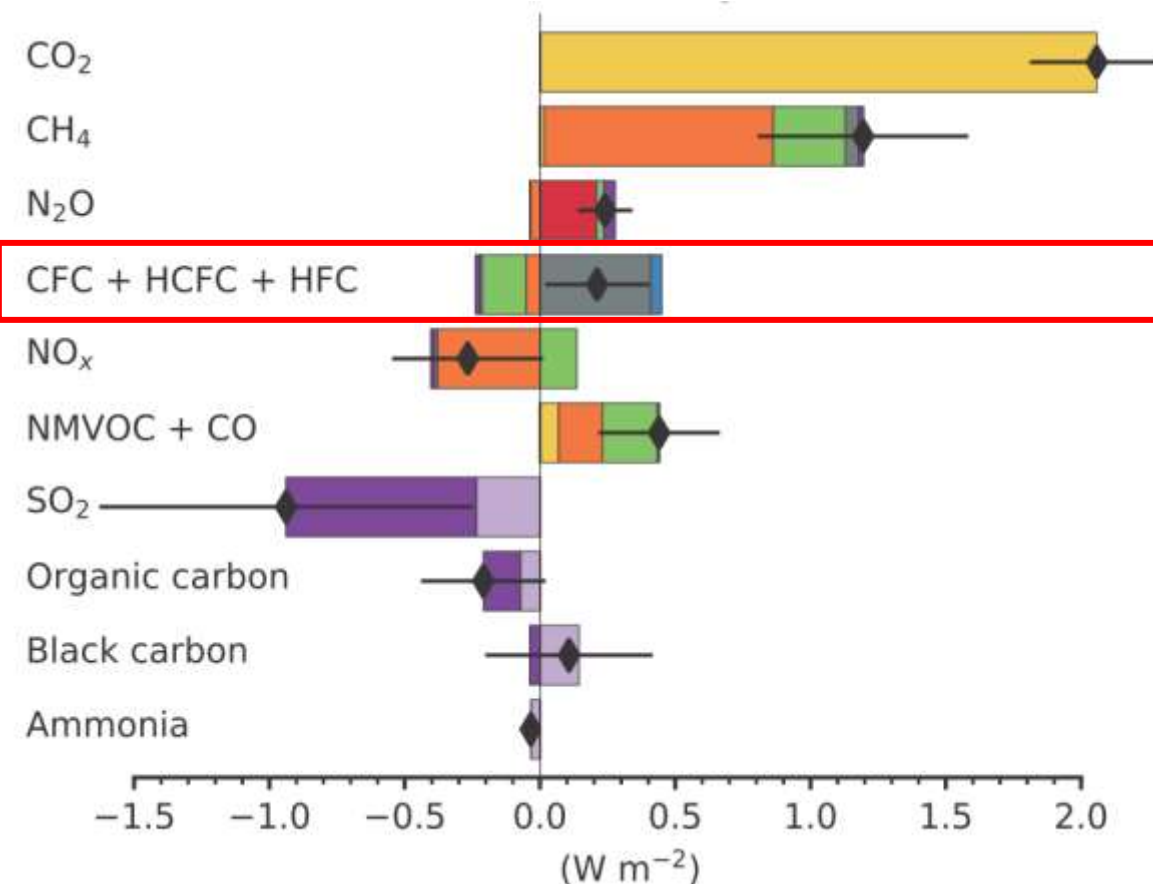
Exploitation of the SR-OLR dataset:

Instantaneous Radiative Efficiency (IRE) or forcing (IRF) of halogenated species.

IRE ($\text{W m}^{-2} \text{ppbv}^{-1}$) = initial radiative flux imbalance in response to an imposed perturbation of a climate driver (e.g. change in [GHG]).

Evaluation of the IRE:

- Today, mostly from radiative transfer model calculations for a few idealized atmospheres.
- Alternative approach directly from the changes in the SR-OLR.



IPCC AR6 WG1 (2021) – chapter 6

IRE of halogenated species

1) Starting point:

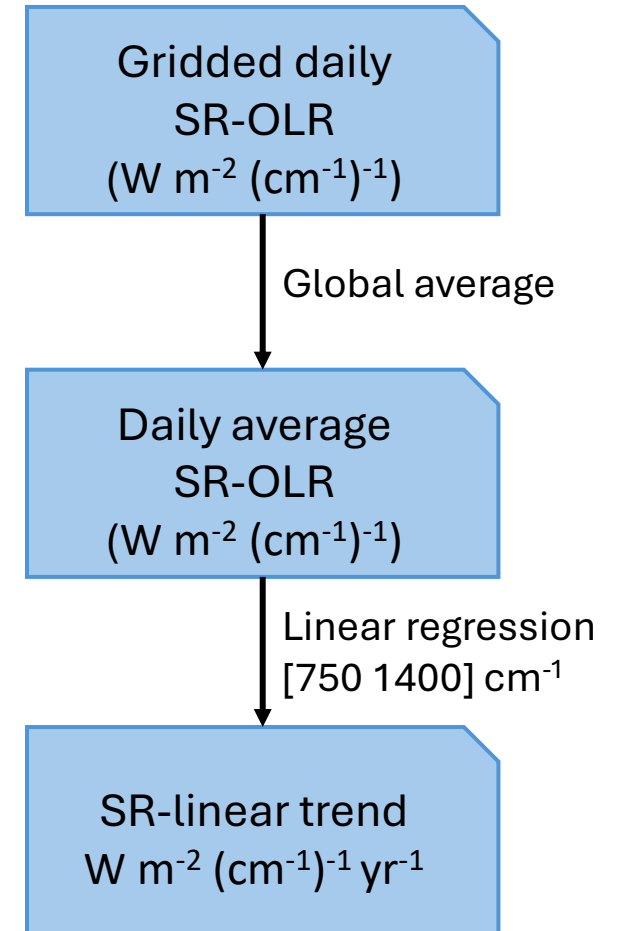
- Clear-sky daily SR-OLR ($2^\circ \times 2^\circ$)
- Between 2008 and 2022 (15 years)
- Between 750 and 1400 cm^{-1} at 0.25 cm^{-1} sampling

2) Global daily average SR-OLR ($\text{W m}^{-2} (\text{cm}^{-1})^{-1}$)

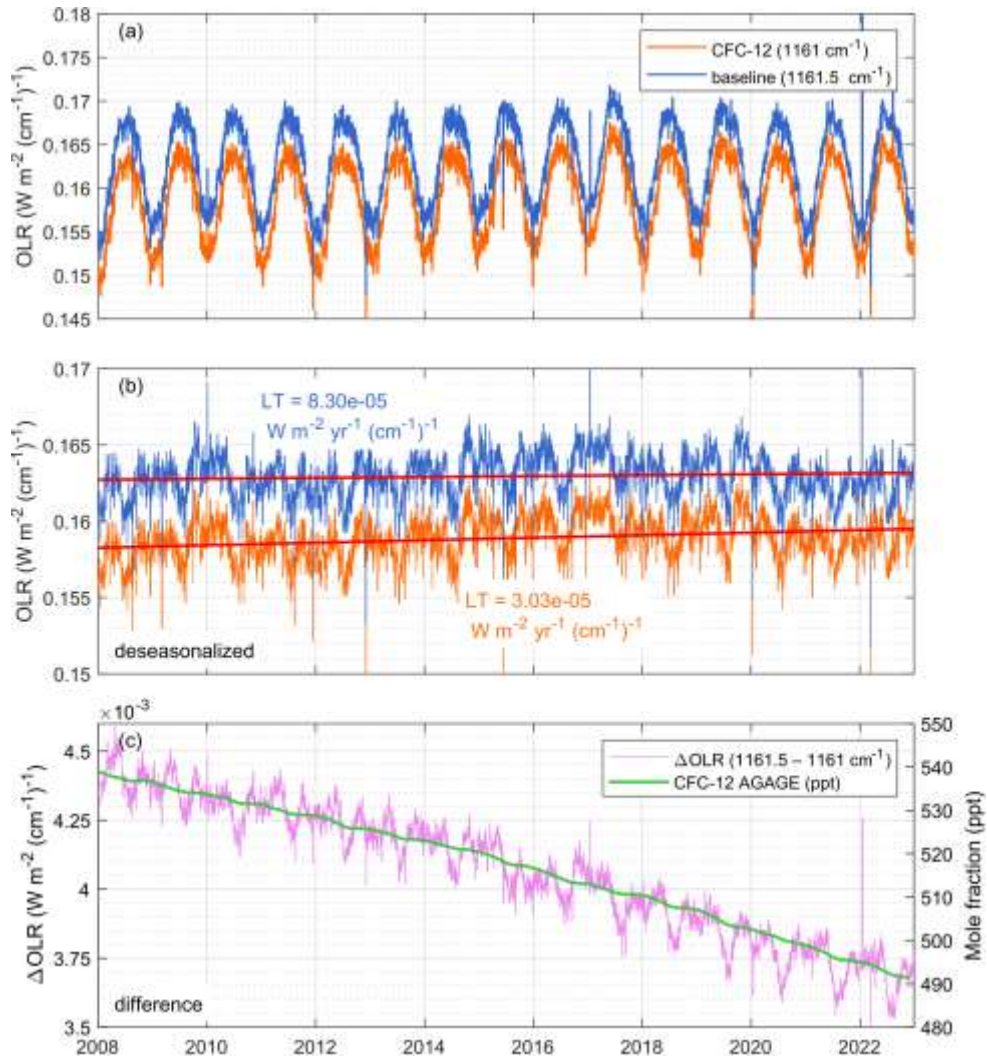
3) For each IASI channel: **Linear trend in the SR-OLR**
($\text{W m}^{-2} (\text{cm}^{-1})^{-1} \text{ year}^{-1}$)

→ Slope of the linear regression:

- **Surface temperature (baseline trend)**
- **Concentration of absorbing species**
 - ↘ [gas] → ↘ absorption → ↗ OLR (compared to baseline)
 - ↗ [gas] → ↗ absorption → ↘ OLR



Example: two IASI channels



OLR time series

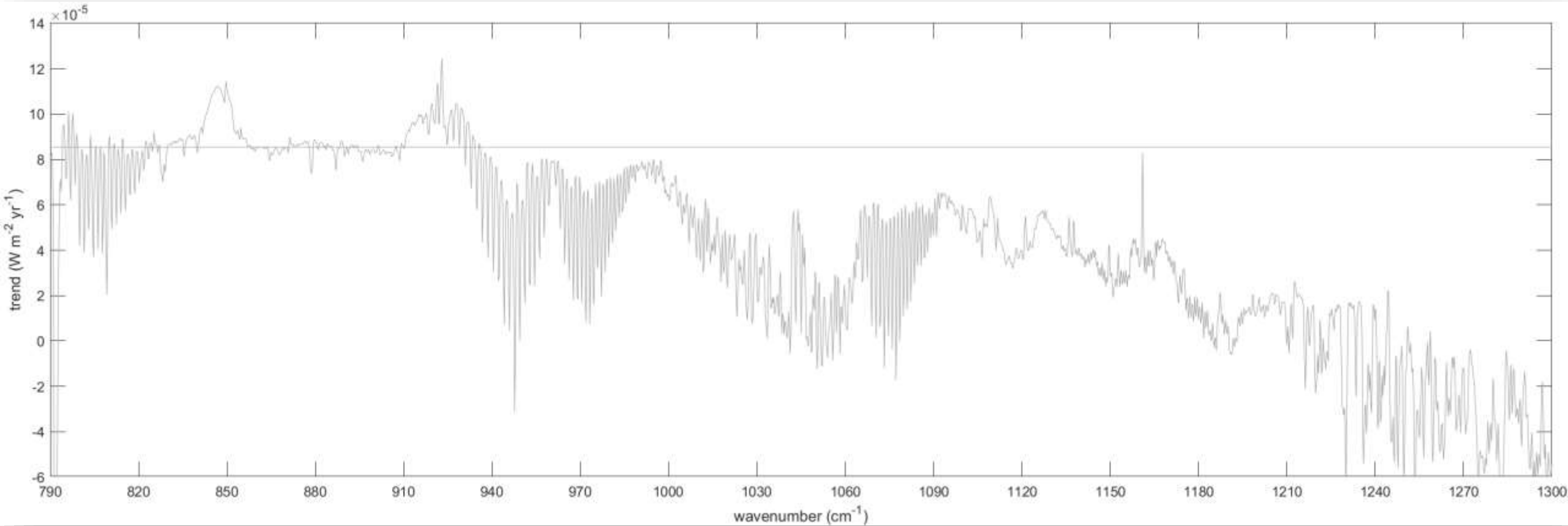
- Baseline channel
- CFC-12 channel

Deseasonalized

Difference

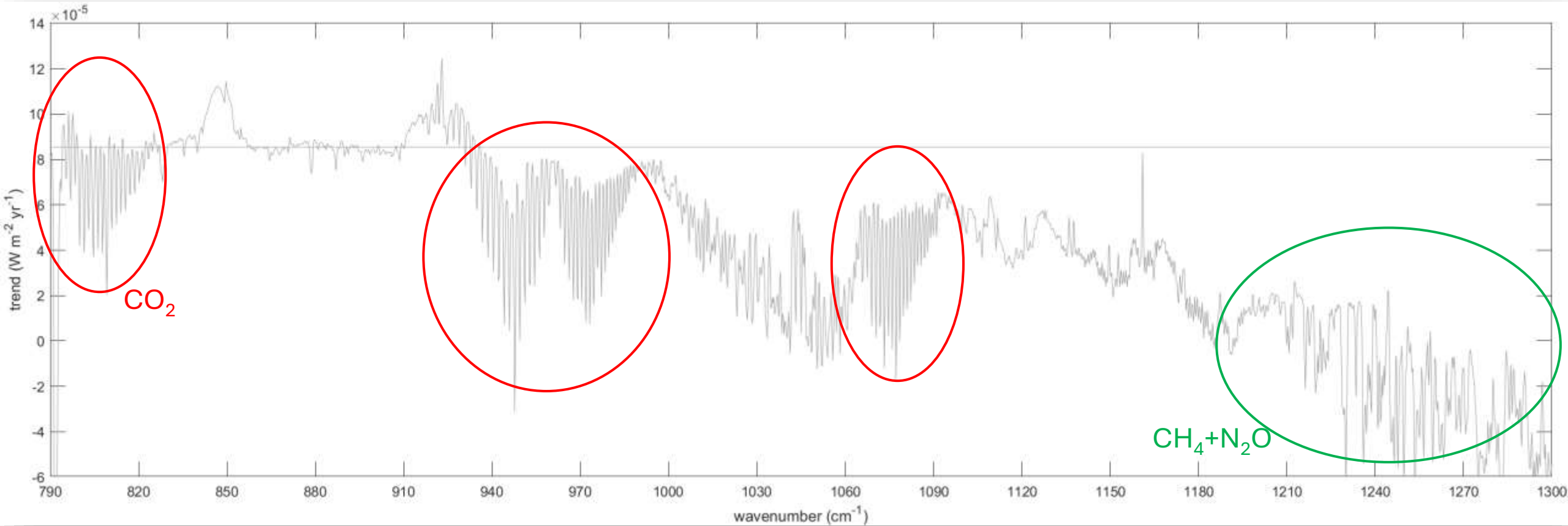
Slope of the linear regression for each IASI channel

- ... from globally averaged daily SR-OLR
- ... between 2008 and 2022
- ... between 750 and 1400 cm^{-1}

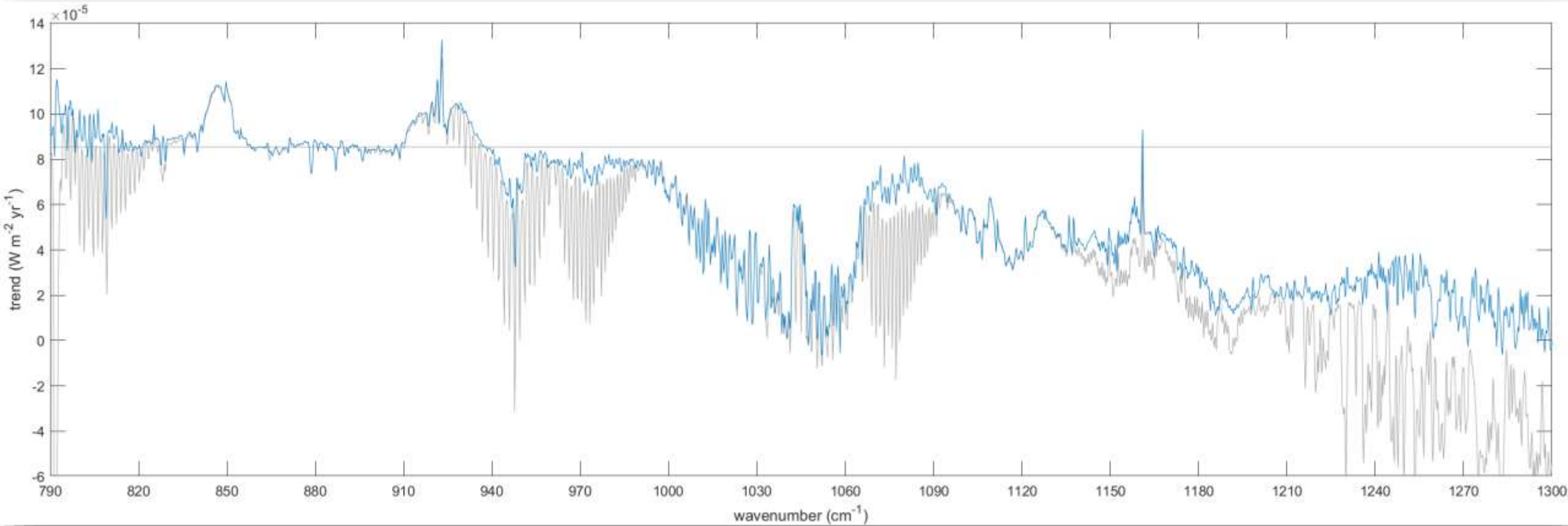


Slope of the linear regression for each IASI channel

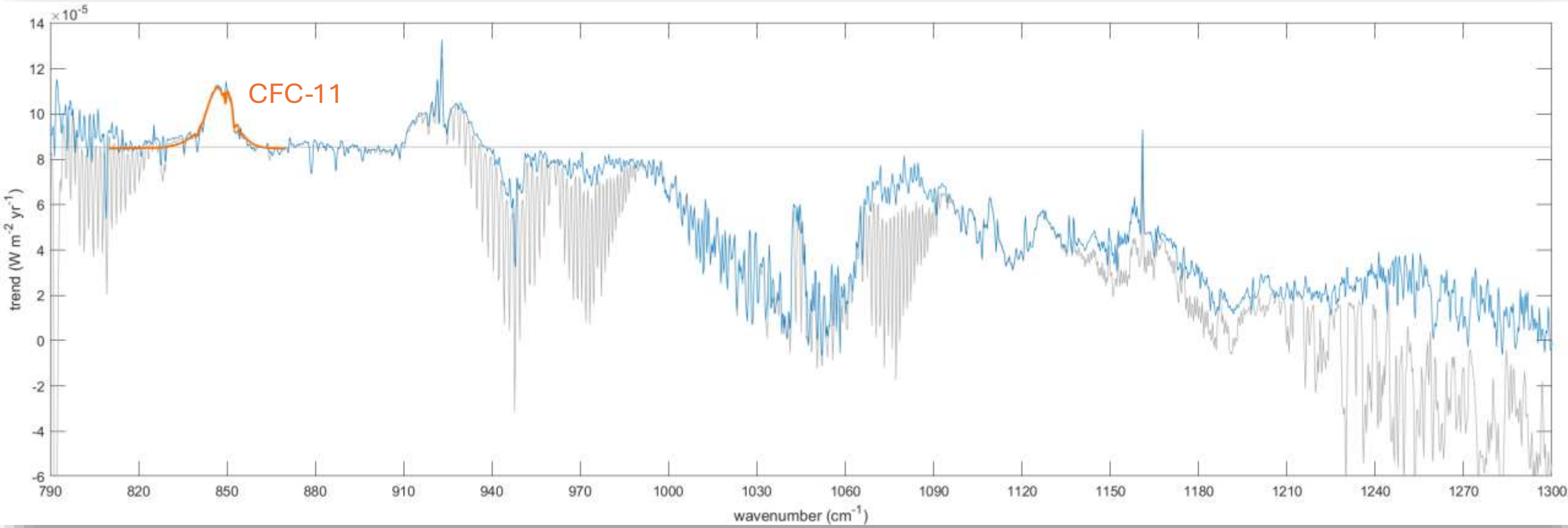
- ... from globally averaged daily SR-OLR
- ... between 2008 and 2022
- ... between 750 and 1400 cm^{-1}



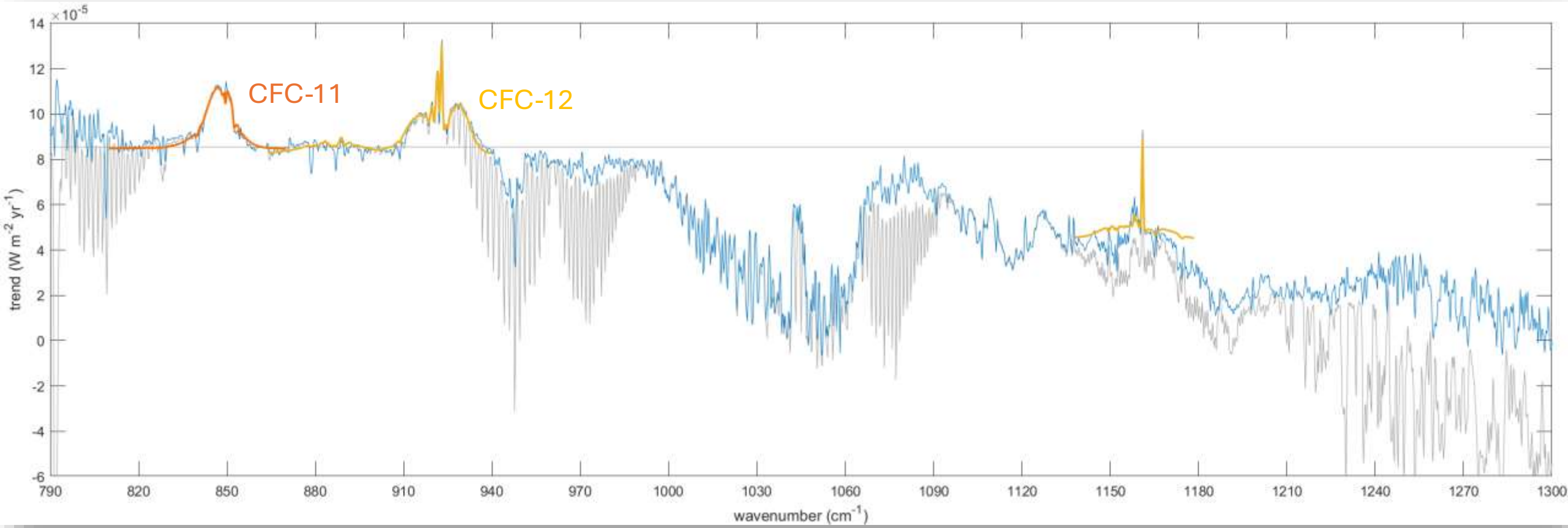
Fit $\text{CO}_2+\text{CH}_4+\text{N}_2\text{O}$ signal and remove their contribution



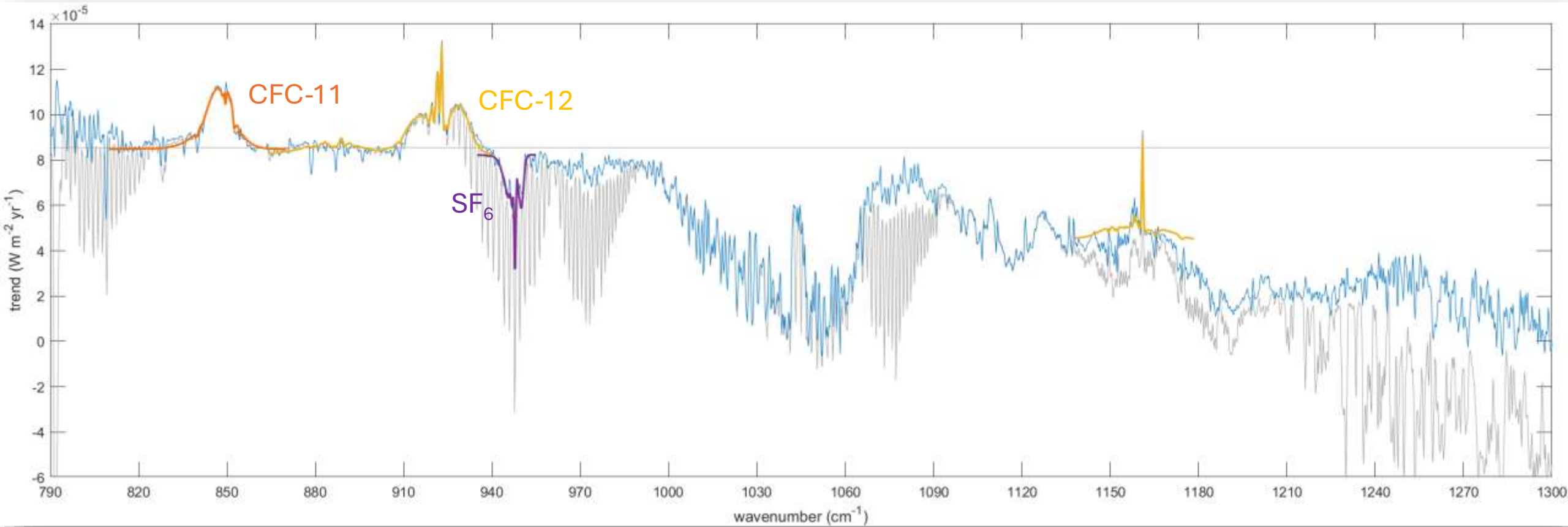
What do we observe ?



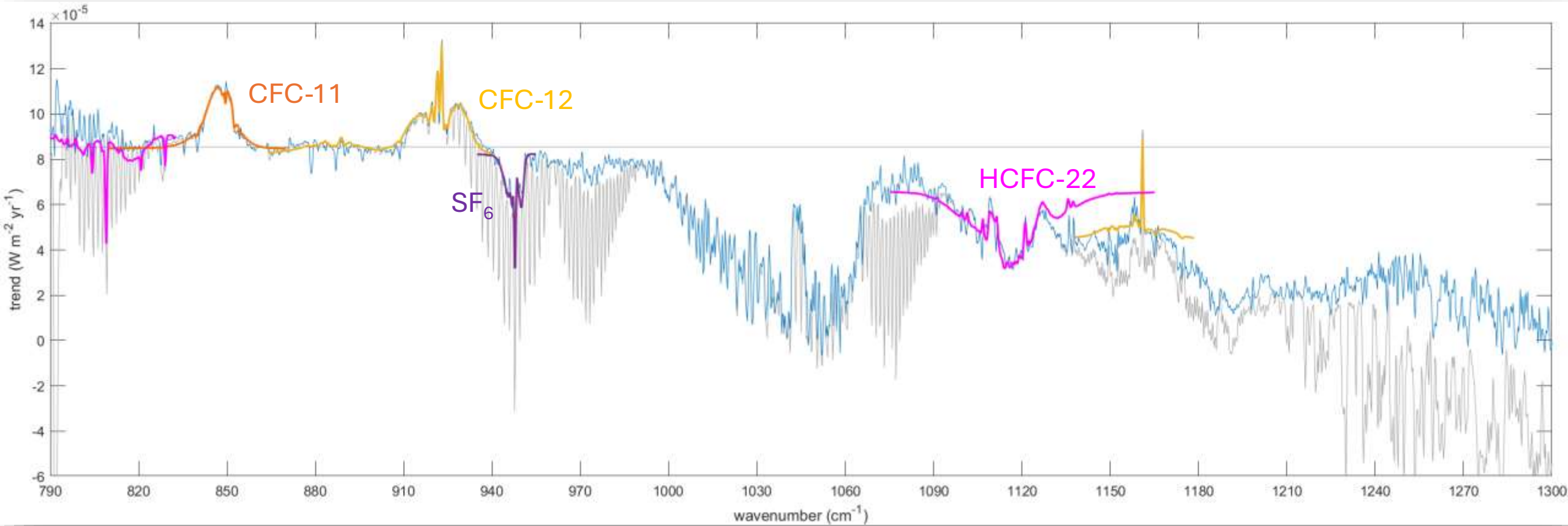
What do we observe ?



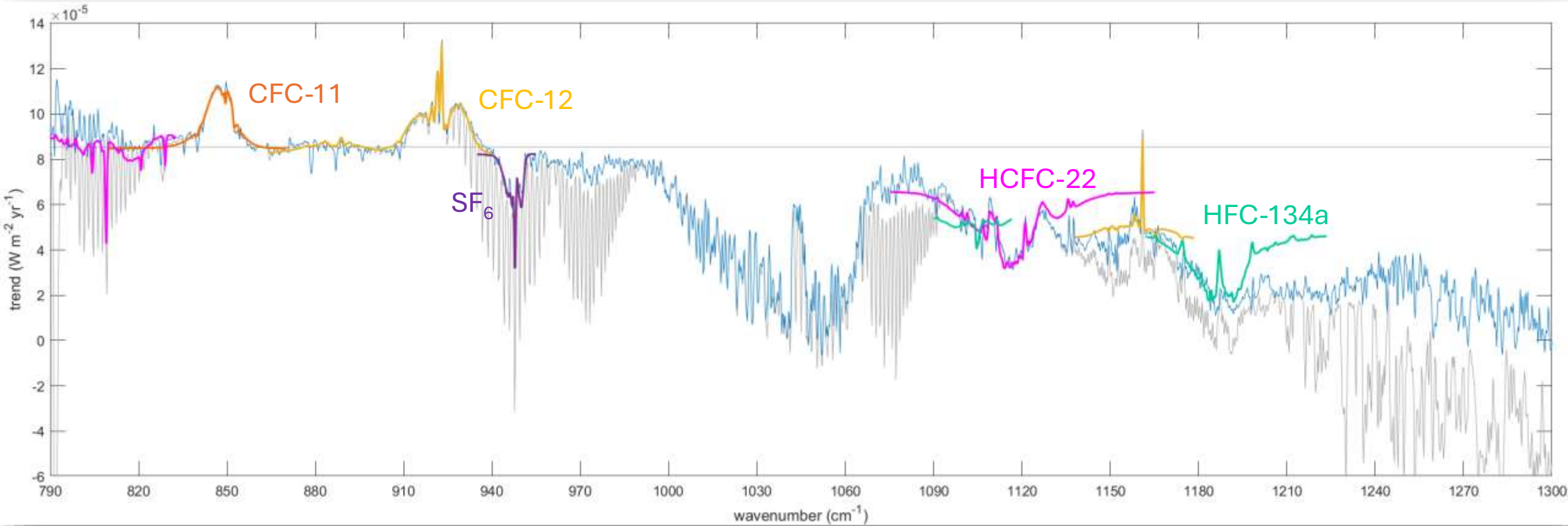
What do we observe ?



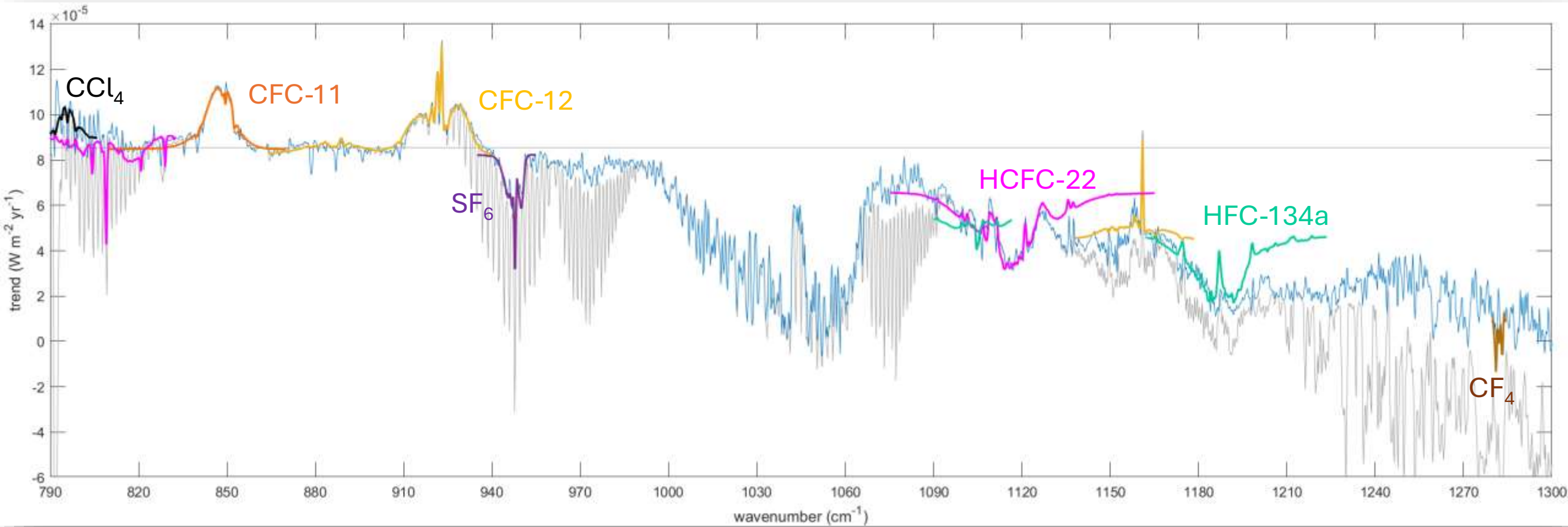
What do we observe ?



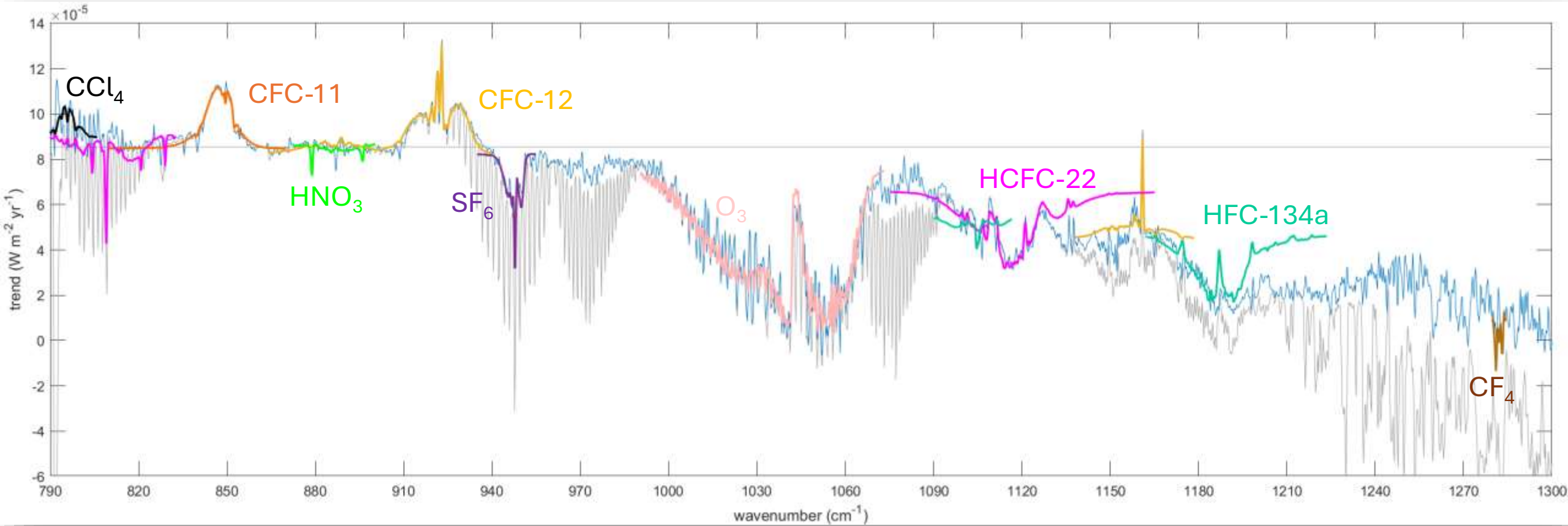
What do we observe ?



What do we observe ?

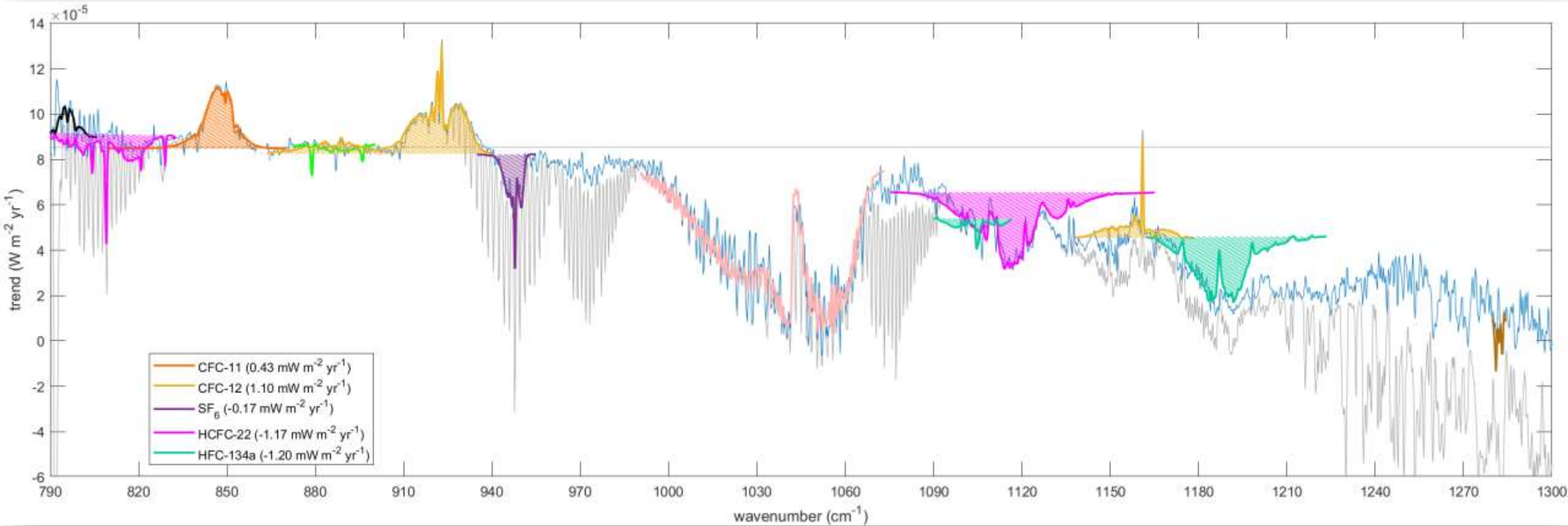


What do we observe ?

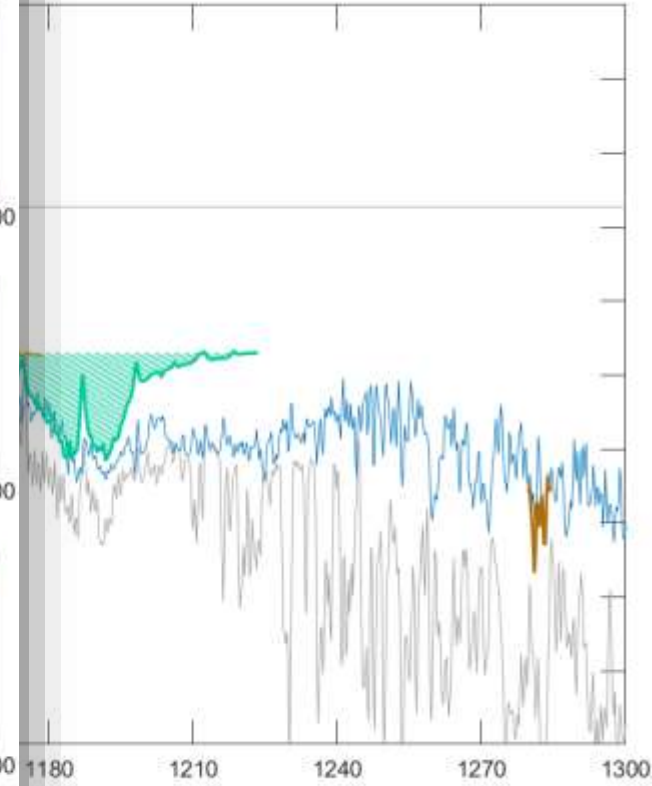
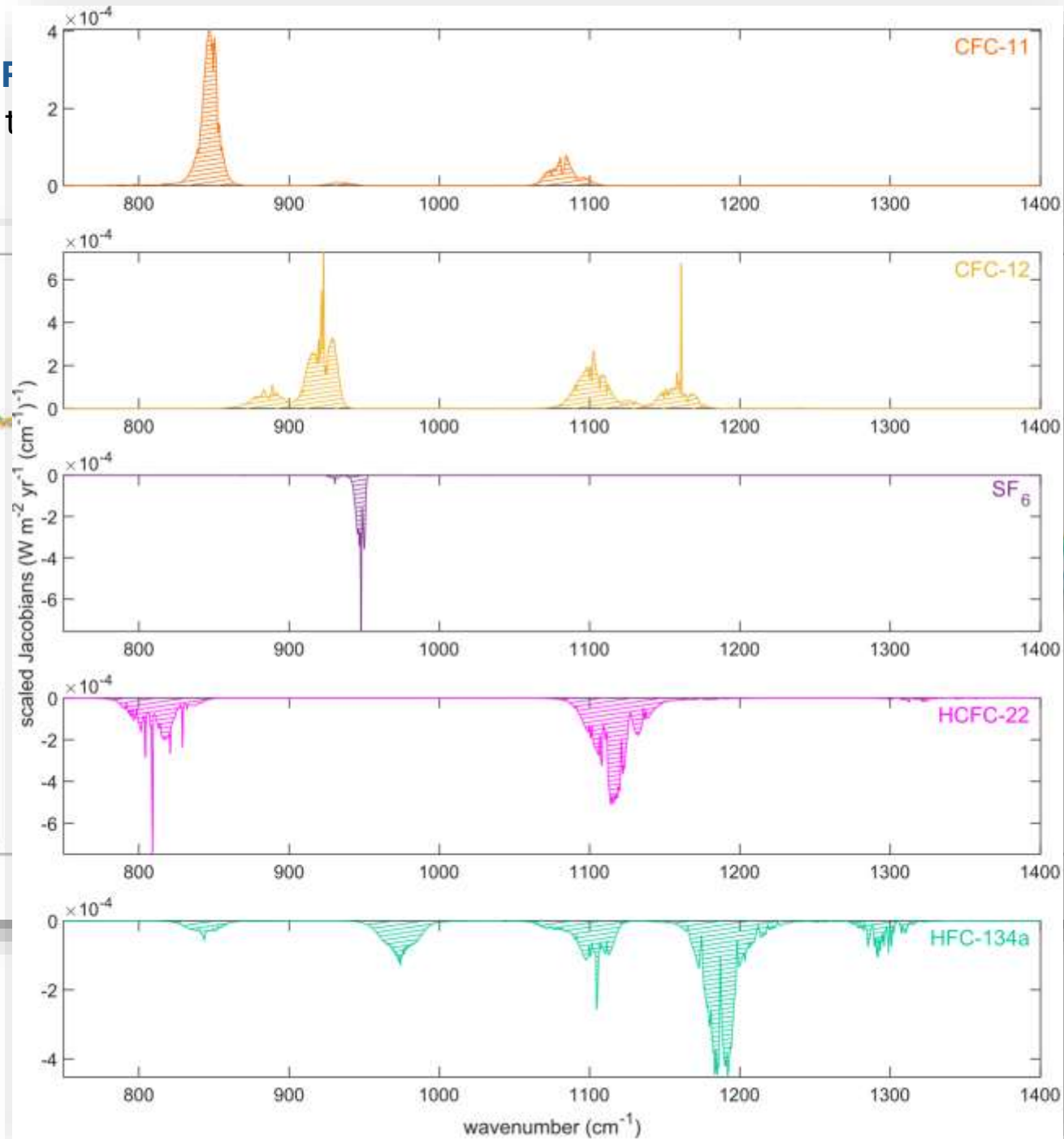
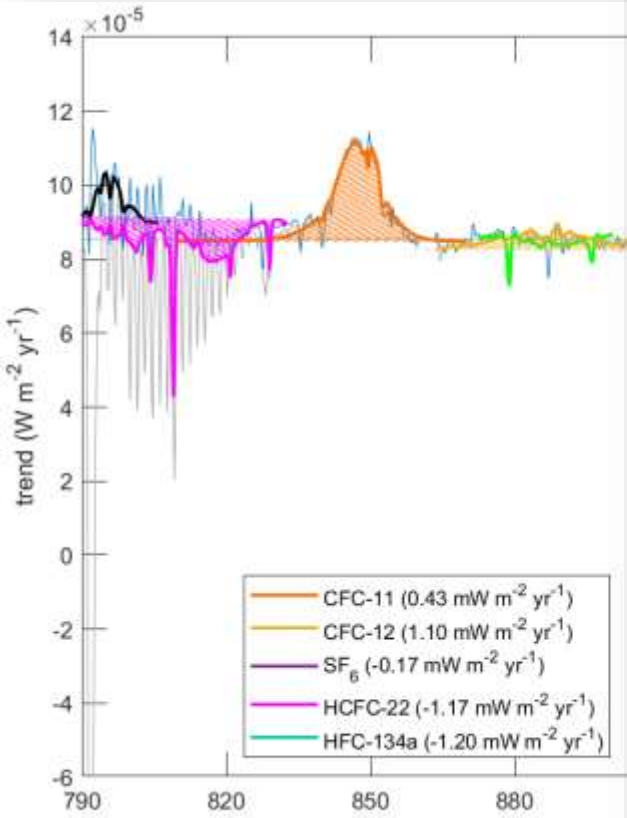


Forcing rate of change (FRC, $\text{W m}^{-2} \text{yr}^{-1}$): CFC-11, CFC-12, SF_6 , HCFC-22 and HFC-134a

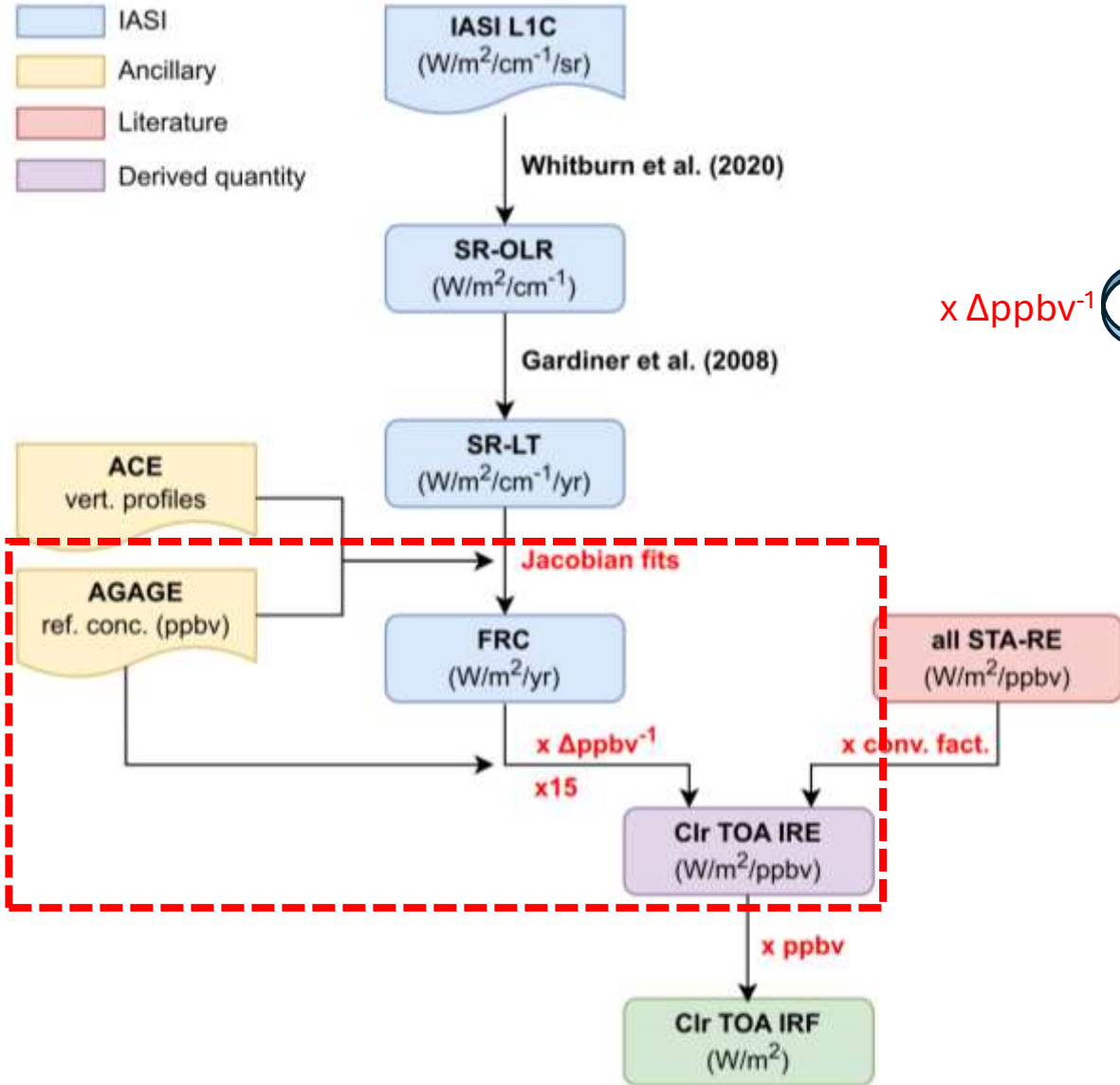
→ Fit, scale and integrate the Jacobian



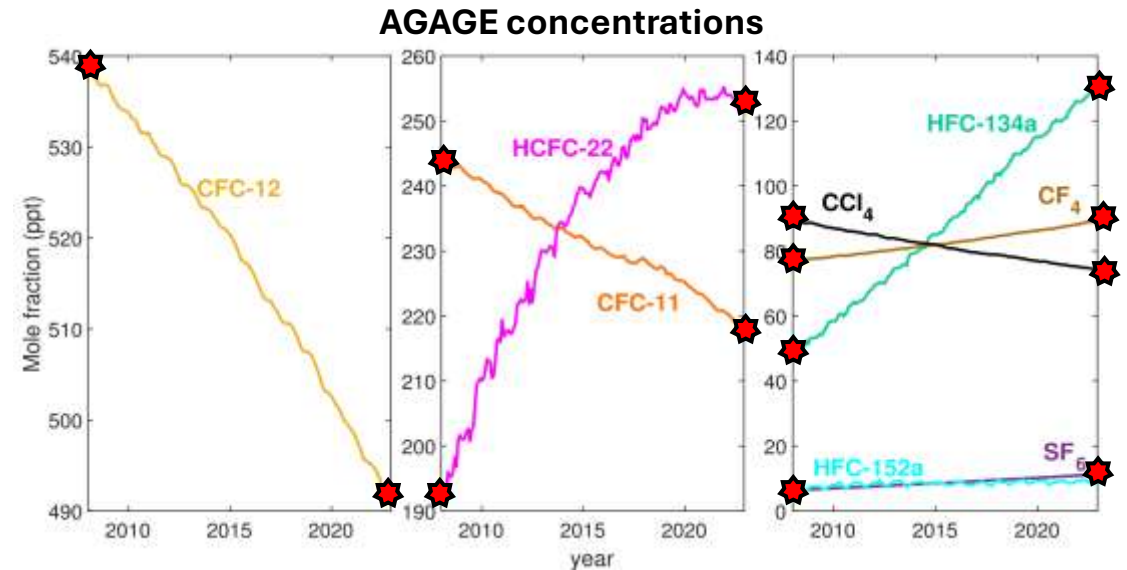
Forcing rate of change (FR)
→ Fit, scale and integrate to



From the FRC ($\text{W m}^{-2} \text{yr}^{-1}$) to the IRE ($\text{W m}^{-2} \text{ppbv}^{-1}$):



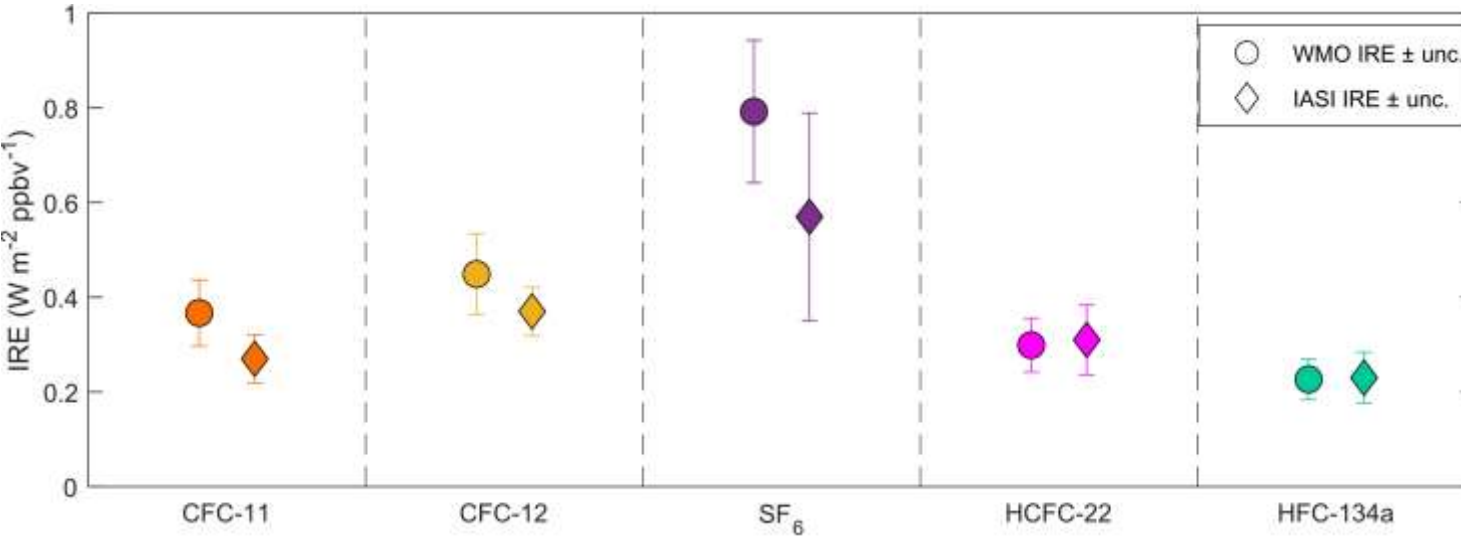
	CFC-11	CFC-12	SF ₆	HCFC-22	HFC-134a
AGAGE 2008 (ppt)	243.5	537.5	6.5	196.2	50.4
AGAGE 2022 (ppt)	219.2	493.0	11.1	253.4	128.2
FRC ($\text{mW m}^{-2} \text{yr}^{-1}$)	0.43	1.10	-0.17	-1.17	-1.20
IRE ($\text{W m}^{-2} \text{ppbv}^{-1}$)	0.27	0.37	0.57	0.31	0.23



Uncertainty budget

	CFC-11	CFC-12	SF ₆	HCFC-22	HFC-134a
Fitting range	5%	11%	21%	14%	12%
Jacobian (cross section)	14%	3%	24%	4%	10%
Jacobian (std. atm.)	4%	5%	4%	1%	5%
Jacobian (ref. year)	0%	0%	1%	0%	0%
Long-term T and H ₂ O changes	0%	0%	0%	5%	5%
Methodology	11%	6%	21%	18%	16%
Total (RSS)	19%	14%	39%	24%	23%

Comparison with modeled IRE



Literature:

- All sky
- Adjusted RE

→ Conversion to TOA IRE

	WMO O ₃ assess. rep. All STA-RE (W m ⁻² ppbv ⁻¹)	Conversion factor (K. Shine)	WMO O ₃ assess. rep. Clr TOA IRE (W m ⁻² ppbv ⁻¹)	IASI Clr TOA IRE (W m ⁻² ppbv ⁻¹)
CFC-11	0.280 ± 0.039	1.31	0.367 ± 0.070	0.27 ± 0.05
CFC-12	0.330 ± 0.0462	1.36	0.422 ± 0.085	0.37 ± 0.05
SF ₆	0.574 ± 0.0804	1.38	0.781 ± 0.151	0.57 ± 0.22
HCFC-22	0.223 ± 0.0312	1.34	0.300 ± 0.057	0.31 ± 0.07
HFC-134a	0.173 ± 0.0242	1.31	0.227 ± 0.043	0.23 ± 0.05

Conclusions and perspectives

- **Alternative approach** for deriving the IRE
- Based on the changes in the SR-OLR
- General good agreement with modeled IREs

Advantages:

- no assumptions on the atmospheric state,
- no need for radiative transfer model calculations

Limitations:

- Absorption in the window region
- Change in concentration

Perspectives:

- IRE of new species with increasing time period of IASI
- IRE of other species outside the window region by fitting simultaneously the interfering species

1 Direct satellite measurements of the radiative forcing of 2 long-lived halogenated gases

3 S. Whitburn^{1,2,*}, L. Clarisse¹, H. De Longueville¹, P.-F. Coheur¹, C. Clerbaux³, and A. Delcloo^{2,4}

4 ¹Spectroscopy, Quantum Chemistry and Atmospheric Remote Sensing (SQUARES), Université libre de Bruxelles (ULB),
5 Brussels, Belgium

6 ²Royal Meteorological Institute of Belgium, Brussels, Belgium

7 ³LATMOS/IPSL, Sorbonne Université, UVSQ, CNRS, Paris, France

8 ⁴Ghent University, Department of Physics and Astronomy, Ghent, Belgium

9 *Corresponding author: Simon Whitburn, simon.whitburn@ulb.be

10 Abstract

11 While the atmospheric concentrations of ozone-depleting chlorofluorocarbons (CFCs) are gradually de-
12 clining following regulatory measures, the levels of other halogenated compounds, such as hydrochlorofluoro-
13 carbons (HCFCs) and sulfur hexafluoride (SF₆) continue to rise or are only just starting to stabilize. Most of
14 these halogenated substances are potent greenhouse gases. Their radiative efficiency, which quantifies their
15 impact on the climate, has until now only been estimated indirectly by means of models. Here, we report
16 the clear-sky instantaneous radiative efficiencies (IRE) of CFC-11, CFC-12, SF₆, HCFC-22 and HFC-134a
17 estimated for the first time directly from experimental data. This is achieved by combing trends observed in
18 15 years (2008–2022) of spectrally resolved infrared radiance fluxes from the Infrared Atmospheric Sounding
19 Interferometer (IASI) satellite sounder, with concentrations measured from ground and space. Comparisons
20 with literature-reported values point to biases of the order of 1 to 31%. The most significant discrepancies
21 are for CFC-11 and SF₆, with our estimates being 31% and 28% lower, respectively.